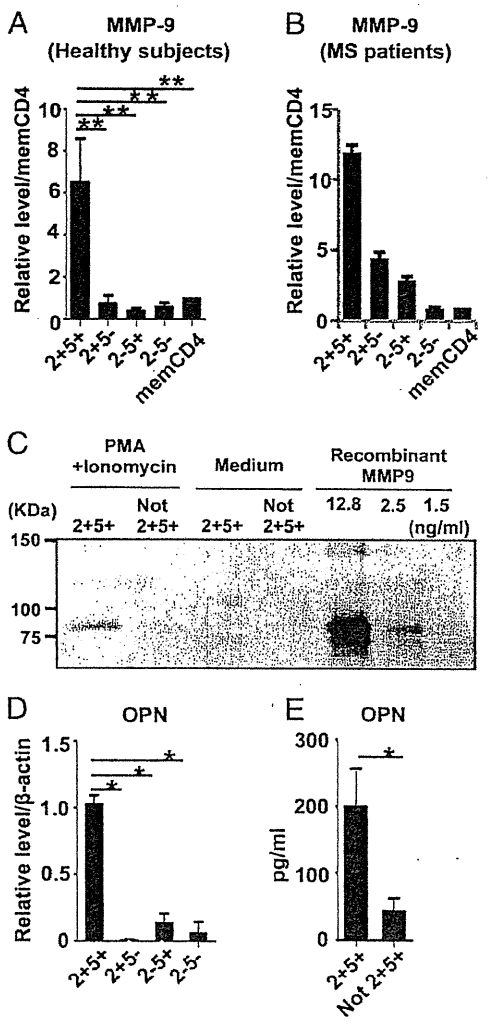

FIGURE 4. CCR2+CCR5+ T cells in the PB have the potential to produce MMP-9 and OPN. Each memory CD4+ T cell subset was isolated from the PBMC of HS (**A**) or MS (**B**) and was stimulated with PMA and ionomycin. Expression levels of MMP-9 mRNA were determined by quantitative RT-PCR. Results were normalized based on the values in unfractionated memory CD4+ T cells. Data represent mean ± SD of four HS or three MS patients. (**C**) CCR2+CCR5+ T cells and CD4+ T cells depleted of CCR2+CCR5+ T cells from HS were stimulated with PMA and ionomycin, and 20 μl of the culture supernatant and recombinant MMP-9 were electrophoresed. Shown are CCR2+CCR5+ T cells activated with PMA and ionomycin (*lane 1*), memory CD4+ T cells depleted of CCR2+CCR5+ T cells activated with PMA and ionomycin (*lane 2*), CCR2+CCR5+ T cells without activation (*lane 3*), memory CD4+ T cells depleted of CCR2+CCR5+ T cells without activation (*lane 4*), and serial dilution of recombinant MMP-9 (*lanes 5–7*). The results shown are representative of three independent experiments. (**D**) Purified memory CD4+ T cell subsets from HS were stimulated with PMA and ionomycin. Expression levels of OPN mRNA were determined by quantitative RT-PCR. Data were normalized to the amount of β-actin mRNA. Data represent mean ± SD of four independent experiments. (**E**) Purified memory CD4+ T cell subsets were stimulated with PMA and ionomycin. OPN concentrations in the supernatants were measured by ELISA. Data represent mean ± SD of four different HS. $*p < 0.05$, $**p < 0.005$.

CCR2+CCR5+ T cells are superior to other T cells in the ability to invade the CNS

Although activated T cells are able to cross the endothelial barrier and enter the CSF compartment relatively easily, the parenchymal basement membrane and the glia limitans would hamper the further entry of the T cells into the CNS parenchyma. Although the endothelial cell basement membrane contains laminin-8 and -10, the parenchymal basal lamina is composed of laminin-1 or -2 (35). It was suggested that leukocyte penetration through the glia limitans requires MMP, such as MMP-2 and MMP-9 (36). After demonstrating that CCR2+CCR5+ T cells have the potential to produce MMP-9, we explored whether CCR2+CCR5+ T cells efficiently invade the CNS parenchyma across the basal lamina and glia limitans. To recapitulate the glia limitans layered with parenchymal basal lamina experimentally, we coated the upper sides of Transwell membrane inserts with laminin-1 or -2 and seeded NHA on the lower sides of the membrane inserts, as described in *Materials and Methods*. When we applied activated T cells to the upper chamber, their migration across the NHA layered with laminin-1 or -2 was less efficient compared with the migration across the untreated membrane or the membrane treated with laminin alone, as assessed by the number of migrated activated T cells collected from the lower chamber (Fig. 5A). Therefore, we assumed that this model would exhibit barrier functions against the penetration of activated T cells. Moreover, we applied CCR2+CCR5+ T cells and memory CD4+ T cells depleted of CCR2+CCR5+ T cells and showed that CCR2+CCR5+ T cells more efficiently penetrated and migrated to the lower chamber compared with the other T cells (Fig. 5B). These results indicate that CCR2+CCR5+ T cells capable of producing MMP-9 and OPN have a greater potential to invade the brain parenchyma.

Table III. Primers used in this study

Primer	5′–3′
MMP1 forward	GATGAAGCAGCCCAGATGTGG
MMP1 reverse	GGAGAGTTGTCCCGATGATC
MMP9 forward	AGCGAGGTGGACCGGATGTTCC
MMP9 reverse	GAGCCCTAGTCCTCAGGGCA
MMP10 forward	GTGTGGAGTTCCTGACGTTGG
MMP10 reverse	GCATCTCTTGGCAAATCTGG
MMP19 forward	CAAGATGTCTCCTGGCTTCC
MMP19 reverse	CGGAGCCCTTAAAGAGGAACAC
MMP28 forward	TGCAGCTGCTACTGTGGGGCCA
MMP28 reverse	TCCAACACGCCGCTGACAGGTAGC
OPN forward	GGCAACGGGGATGGCCTTGT
OPN reverse	TTTTCCACGGACCTGCCAGCAAC
β-actin forward	CACTCTTCCAGCCTTCCTTCC
β-actin reverse	GCGTACAGGTCTTTGCGGATG
IFN-γ forward	CAGGTCATTCAGATGTAGCG
IFN-γ reverse	GCTTTTCGAAGTCATCTCG
IL-17 forward	CCAGGATGCCCAAATTCTGAGGAC
IL-17 reverse	CAAGGTGAGGTGGATCGGTTGTAG
RORC forward	AGAAGGACAGGGAGCCAAGG
RORC reverse	GTGATAACCCCGTAGTGGATC
T-bet forward	TCAGGGAAAGGACTCACCTG
T-bet reverse	AATAGCCTCCCCCATTCAAA

CCR2+CCR5+CCR6− subset producing IFN-γ and MMP-9 is selectively enriched in the CSF in MS

We noticed that CCR2+CCR5+ T cells consist of CCR6+ and CCR6− subset (Supplemental Fig. 1). Because Th17 cells appear to be enriched in CCR6+ T cells, we were interested to know whether CCR2+CCR5+ T cells could be functionally divided based on the expression of CCR6. When we compared the frequency of CCR2+CCR5+CCR6+ and CCR2+CCR5+CCR6− T cells between PB and CSF, the frequency of CCR6− subset was much higher in the CSF of MS in relapse than in PB ($p < 0.0005$), whereas the CCR6+ subset was not (Fig. 6A). Further analyses revealed that expression levels of IFN-γ in the CCR6− subset were higher than those in the CCR6+ subset, as assessed by RT-PCR (Fig. 6B). In contrast, the CCR6+ subset expressed much

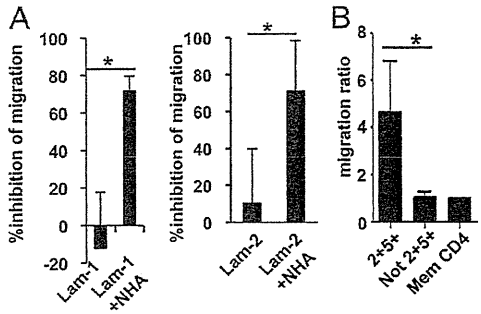

FIGURE 5. T cell migration across an in vitro glia limitans model. (**A**) The upper sides of Transwell membrane inserts were coated with laminin-1 (Lam-1; *left panel*) or laminin-2 (Lam-2; *right panel*), and NHA were seeded on the lower sides of the membrane inserts, as described in *Materials and Methods*. Unfractionated T cells isolated from PBMC were stimulated with PMA and ionomycin for 18 h and seeded onto the upper chambers. Eight hours later, absolute numbers of migrated cells were counted by flow cytometry. Data shown are the percentage inhibition of the migration, calculated as follows: [(migrated cell number through uncoated membrane) − (migrated cell number through membrane coated with laminin alone or laminin and NHA)] × 100/(migrated cell number through uncoated membrane). Data represent mean ± SD of four independent experiments. (**B**) PBMC from HS were sorted into memory $CD4^+CCR2^+CCR5^+$ T cells (2+5+), memory $CD4^+$ T cells depleted of $CCR2^+CCR5^+$ T cells (Not 2+5+), and unfractionated memory $CD4^+$ T cells (Mem CD4) by flow cytometry. The cells were stimulated with plate-bound anti-CD3/CD28 mAb for 60 h and seeded onto the upper chambers, whose membranes were coated with laminin-2 and NHA, as described in (A). Eight hours later, absolute numbers of migrated cells were counted by flow cytometry. To normalize individual variance, data are expressed as migration ratio of the number of migrated cells/number of migrated unfractionated memory $CD4^+$ T cells. Data represent mean ± SD of four independent experiments. $*p < 0.05$.

higher levels of IL-17 and RORC compared with the $CCR6^-$ subset. We also measured expression levels of MMP-9 mRNA; a much higher level of MMP-9 mRNA was found in the $CCR6^-$ subset (individual relative expression level from two samples = 1.0257 and 0.1127306) compared with the $CCR6^+$ subset (individual relative expression level = 0.0185 and 0.00345). Taken together, we postulate that $CCR2^+CCR5^+CCR6^-$ T cells producing IFN-γ, but not $CCR2^+CCR5^+CCR6^+$ T cells, play a crucial role in triggering the relapse of MS and expand in the CSF during relapse.

Discussion

Chemokines are a family of small chemotactic cytokines, which is a key to understanding the immune homeostasis, self-defense, and inflammation. Interactions between chemokines and their receptors are crucial for the migration of lymphocyte populations, such as T cells, macrophages, dendritic cells, and neutrophils, in autoimmune diseases, allergy, and cancer (37). Although chemokine receptor expression by the CSF lymphocytes or by brain-infiltrating T cells has been repeatedly investigated with regard to the pathogenesis of MS (38), most of the previous studies did not analyze the proportional changes of T cells simultaneously expressing more than two chemokine receptors. We showed that memory $CD4^+$ T cells expressing both CCR2 and CCR5 are selectively enriched in the CSF in MS during relapse but not in NIND or OIND.

Both CCR2 and CCR5 belong to the CC family of chemokines, which have two adjacent cysteines close to their N terminus. CCR2 binds CCL2 (MCP-1), CCL7 (MCP-3), CCL11 (eotaxin), CCL13 (MCP-4), and CCL16 (LEC), whereas CCR5 binds CCL3 (MIP-1α), CCL4 (MIP-1β), CCL5 (RANTES), CCL8, CCL11, CCL13, and CCL14. Among these chemokines, CCL5 was increased in the CSF in MS during acute relapses (39), and overexpression of CCL3 was detected in the brain tissues from MS (40). In contrast, CCL2 was decreased in the CSF in MS during relapses (38, 41), and this could be the result of consumption by $CCR2^+$ cells (42). Moreover, the presence of CCL2 and CCL5 was recently demonstrated in endothelial cells in brain samples from MS (43). CCL2 and CCL5 appear to play a critical role in adhesions of the encephalitogenic T cells to brain endothelial cells in a model of EAE (44). More recently, CCL2–CCR2 pairs were shown to play a critical role in the transendothelial migration of effector $CD4^+$ T cells (45), suggesting the importance of CCR2 expression for BBB transmigration. Taking these into consideration, we postulate that the chemokine gradient would facilitate the adherence of $CCR2^+CCR5^+$ T cells to the endothelial cells, as well as T cell entry into the CNS parenchyma during relapses of MS. Interestingly, $CCR2^-CCR5^+$ T cells, which produce a large quantity of IFN-γ, were also enriched in the CSF in MS. However, it was not specific for MS but was also present in the patients with NIND (Fig. 1C), indicating that only $CCR2^+CCR5^+$ T cells are specifically involved in the autoimmune pathology of MS. We subsequently found that the $CCR2^+CCR5^+$ T cells have an exceptional ability to produce MMP-9, an enzyme that is capable of disrupting the glia limitans, which led us to speculate that they have the

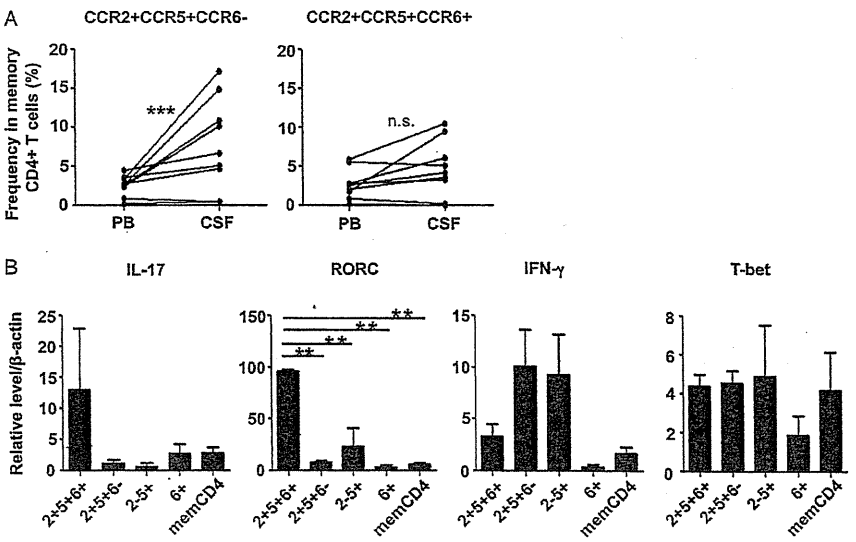

FIGURE 6. $CCR2^+CCR5^+CCR6^-$ T cells, but not $CCR2^+CCR5^+CCR6^+$ T cells, were enriched in the CSF of MS in relapse. (**A**) Cells were stained, as described in Fig. 1C, and frequencies of $CCR2^+CCR5^+CCR6^-$ and $CCR2^+CCR5^+CCR6^-$ T cells in the CSF and PB from nine MS patients in relapse were examined. Lines connect data from paired CSF and PB samples from the same patients. (**B**) Each memory $CD4^+$ T cell subset was isolated from the PBMC of HS and stimulated with PMA and ionomycin for 18 h. Expression levels of IL-17, IFN-γ, RORC, and T-bet mRNA were determined by quantitative RT-PCR. Data represent mean ± SD of three independent experiments. $**p < 0.005$, $***p < 0.0005$. n.s., Not significant.

potential to destroy the integrity of the BBB and trigger the cascade of inflammatory pathology. The MMP-9–producing CCR2+ CCR5+ T cells were indeed superior to the other T cells in their ability to cross the in vitro model of glia limitans layered by laminin-1 or -2.

MMP-9 appears to play a major role in EAE by disrupting the glia limitans, and a specific substrate of MMP-9 was shown to be dystroglycan, anchoring astrocyte end feet to parenchymal basement membrane via interaction with laminin-1 and -2 (36). Laminin-1 and -2 constitute the major laminin isoforms present in the CNS parenchymal basal lamina (35). Taken together, we postulate that the distinguished ability to produce MMP-9 would license the CCR2+CCR5+ T cells to serve as early invaders into the CNS parenchyma during relapses of MS. The CCR2+CCR5+ T cells also produce a large amount of OPN, an integrin-binding protein abundantly expressed in active MS lesions (33). OPN is a pleiotropic protein that interacts with various integrins. In addition to its function as an adhesion molecule, OPN promotes the survival of activated T cells and the production of proinflammatory cytokines by APC (46). It is very likely that paracrine OPN produced by the CCR2+CCR5+ T cells would promote the survival of these MMP-9–producing T cells in the CNS, which leads to further enrichment of the CCR2+CCR5+ T cells in the CSF.

Seeing the specific increase in the CCR2+CCR5+ T cells in the CSF in MS, we were very curious to know whether this T cell population is enriched with autoimmune T cells critical for the initiation of MS pathology. By stimulating the PB CCR2+CCR5+ T cells with MBP, we showed that, in patients with MS relapse, this T cell subset produces a large quantity of IFN-γ and some IL-17 in response to MBP, a representative autoantigen for MS (Fig. 3C). In contrast, the cells from MS in remission or from healthy controls did not respond significantly. Although we did not examine the CSF T cells' response to MBP because of a technical difficulty, it is likely that the CCR2+CCR5+ T cells in the CSF in MS during relapse are enriched with MBP-reactive autoimmune T cells as well.

Of note, Zhang et al. (47) recently reported that CCR2+CCR5+ cells are highly differentiated, yet stable, effector ~~memory~~ ~~CD4~~+ T cells equipped for provoking rapid recall response. They showed evidence that CCR2+CCR5+ T cells should have undergone reactivation and subsequent proliferation more often than other memory T cell subsets and are resistant to apoptosis. Thus, it is likely that autoreactive T cells are enriched in CCR2+CCR5+ T cells that have survived following repeated reactivation over a long period of time. We assume that once autoreactive T cells differentiate into stable effector memory T cells expressing CCR2 and CCR5, they might persist and trigger relapse repeatedly. We further revealed that the CCR6−, but not the CCR6+, subset of CCR2+CCR5+ T cells was significantly enriched in the CSF of MS patients during relapse.

Reboldi et al. (48) reported that CCR6+ T cells are more enriched in CSF than in the PB of clinically isolated syndrome (CIS). Diagnosis of CIS can be made when patients developed a single attack of neurologic disability that is consistent with demyelinating pathology and that may turn out to be the first episode of MS (49). However, in our Japanese patients having clinically definite MS, we did not detect enrichment of CCR6+ T cells in the CSF. Rather, T cells bearing Th17 phenotypes appeared to be prohibited from entry into the CNS in MS. The difference between the results in CIS and MS could be explained by the premise that autoimmune pathology may be premature at the CIS stage. In contrast, the increase in CCR2+CCR5+ T cells in the CSF was not detected in the patients who had MS for >10 y. These observations are in accordance with the postulate that acquired and innate immune components, as well as neurodegenerative components, differentially contribute to the different stages of MS (50).

In summary, we identified a unique CCR2+CCR5+CCR6− T cell population that is enriched in the CSF of patients with exacerbated MS. Our data suggest that targeting this population may be a novel therapeutic approach for MS.

Acknowledgments

We thank Dr. Britta Engelhardt for valuable comments and Hiromi Yamaguchi and Ryoko Saga for excellent technical assistance.

Disclosures

The authors have no financial conflicts of interest.

References

1. McFarland, H. F., and R. Martin. 2007. Multiple sclerosis: a complicated picture of autoimmunity. *Nat. Immunol.* 8: 913–919.
2. Trapp, B. D., and K. A. Nave. 2008. Multiple sclerosis: an immune or neurodegenerative disorder? *Annu. Rev. Neurosci.* 31: 247–269.
3. Wucherpfennig, K. W., and J. L. Strominger. 1995. Molecular mimicry in T cell-mediated autoimmunity: viral peptides activate human T cell clones specific for myelin basic protein. *Cell* 80: 695–705.
4. Hur, E. M., S. Youssef, M. E. Haws, S. Y. Zhang, R. A. Sobel, and L. Steinman. 2007. Osteopontin-induced relapse and progression of autoimmune brain disease through enhanced survival of activated T cells. *Nat. Immunol.* 8: 74–83.
5. Ransohoff, R. M., P. Kivisäkk, and G. Kidd. 2003. Three or more routes for leukocyte migration into the central nervous system. *Nat. Rev. Immunol.* 3: 569–581.
6. Bartholomäus, I., N. Kawakami, F. Odoardi, C. Schläger, D. Miljkovic, J. W. Ellwart, W. E. Klinkert, C. Flügel-Koch, T. B. Issekutz, H. Wekerle, and A. Flügel. 2009. Effector T cell interactions with meningeal vascular structures in nascent autoimmune CNS lesions. *Nature* 462: 94–98.
7. Gijbels, K., R. E. Galardy, and L. Steinman. 1994. Reversal of experimental autoimmune encephalomyelitis with a hydroxamate inhibitor of matrix metalloproteases. *J. Clin. Invest.* 94: 2177–2182.
8. Engelhardt, B. 2010. T cell migration into the central nervous system during health and disease: Different molecular keys allow access to different central nervous system compartments. *Clin. Exp. Neuroimmunol.* 1: 79–93.
9. Steinman, L. 2009. Shifting therapeutic attention in MS to osteopontin, type 1 and type 2 IFN. *Eur. J. Immunol.* 39: 2358–2360.
10. Aranami, T., and T. Yamamura. 2008. Th17 Cells and autoimmune encephalomyelitis (EAE/MS). *Allergol. Int.* 57: 115–120.
11. Tzartos, J. S., M. A. Friese, M. J. Craner, J. Palace, J. Newcombe, M. M. Esiri, and L. Fugger. 2008. Interleukin-17 production in central nervous system-infiltrating T cells and glial cells is associated with active disease in multiple sclerosis. *Am. J. Pathol.* 172: 146–155.
12. Kebir, H., I. Ifergan, J. I. Alvarez, M. Bernard, J. Poirier, N. Arbour, P. Duquette, and A. Prat. 2009. Preferential recruitment of interferon-gamma-expressing TH17 cells in multiple sclerosis. *Ann. Neurol.* 66: 390–402.
13. Panitch, H. S., R. L. Hirsch, A. S. Haley, and K. P. Johnson. 1987. Exacerbations of multiple sclerosis in patients treated with gamma interferon. *Lancet* 1: 893–895.
14. Broux, B., K. Pannemans, X. Zhang, S. Markovic-Plese, T. Broekmans, B. O. Eijnde, B. Van Wijmeersch, V. Somers, P. Geusens, S. van der Pol, et al. 2012. CX(3)CR1 drives cytotoxic CD4(+)CD28(−) T cells into the brain of multiple sclerosis patients. *J. Autoimmun.* 38: 10–19.
15. Saxena, A., G. Martin-Blondel, L. T. Mars, and R. S. Liblau. 2011. Role of CD8 T cell subsets in the pathogenesis of multiple sclerosis. *FEBS Lett.* 585: 3758–3763.
16. Segal, B. M., C. S. Constantinescu, A. Raychaudhuri, L. Kim, R. Fidelus-Gort, and L. H. Kasper; Ustekinumab MS Investigators. 2008. Repeated subcutaneous injections of IL12/23 p40 neutralising antibody, ustekinumab, in patients with relapsing-remitting multiple sclerosis: a phase II, double-blind, placebo-controlled, randomised, dose-ranging study. *Lancet Neurol.* 7: 796–804.
17. Mackay, C. R. 2001. Chemokines: immunology's high impact factors. *Nat. Immunol.* 2: 95–101.
18. Proudfoot, A. E. 2002. Chemokine receptors: multifaceted therapeutic targets. *Nat. Rev. Immunol.* 2: 106–115.
19. Izikson, L., R. S. Klein, I. F. Charo, H. L. Weiner, and A. D. Luster. 2000. Resistance to experimental autoimmune encephalomyelitis in mice lacking the CC chemokine receptor (CCR)2. *J. Exp. Med.* 192: 1075–1080.
20. Sallusto, F., and A. Lanzavecchia. 2000. Understanding dendritic cell and T-lymphocyte traffic through the analysis of chemokine receptor expression. *Immunol. Rev.* 177: 134–140.
21. Nagata, K., K. Tanaka, K. Ogawa, K. Kemmotsu, T. Imai, O. Yoshie, H. Abe, K. Tada, M. Nakamura, K. Sugamura, and S. Takano. 1999. Selective expression

of a novel surface molecule by human Th2 cells in vivo. *J. Immunol.* 162: 1278–1286.
22. Ransohoff, R. M. 2009. Chemokines and chemokine receptors: standing at the crossroads of immunobiology and neurobiology. *Immunity* 31: 711–721.
23. Acosta-Rodriguez, E. V., L. Rivino, J. Geginat, D. Jarrossay, M. Gattorno, A. Lanzavecchia, F. Sallusto, and G. Napolitani. 2007. Surface phenotype and antigenic specificity of human interleukin 17-producing T helper memory cells. *Nat. Immunol.* 8: 639–646.
24. Sato, W., T. Aranami, and T. Yamamura. 2007. Cutting edge: Human Th17 cells are identified as bearing CCR2+CCR5− phenotype. *J. Immunol.* 178: 7525–7529.
25. Singh, S. P., H. H. Zhang, J. F. Foley, M. N. Hedrick, and J. M. Farber. 2008. Human T cells that are able to produce IL-17 express the chemokine receptor CCR6. *J. Immunol.* 180: 214–221.
26. McDonald, W. I., A. Compston, G. Edan, D. Goodkin, H. P. Hartung, F. D. Lublin, H. F. McFarland, D. W. Paty, C. H. Polman, S. C. Reingold, et al. 2001. Recommended diagnostic criteria for multiple sclerosis: guidelines from the International Panel on the diagnosis of multiple sclerosis. *Ann. Neurol.* 50: 121–127.
27. Takahashi, K., T. Aranami, M. Endoh, S. Miyake, and T. Yamamura. 2004. The regulatory role of natural killer cells in multiple sclerosis. *Brain* 127: 1917–1927.
28. Leppert, D., J. Ford, G. Stabler, C. Grygar, C. Lienert, S. Huber, K. M. Miller, S. L. Hauser, and L. Kappos. 1998. Matrix metalloproteinase-9 (gelatinase B) is selectively elevated in CSF during relapses and stable phases of multiple sclerosis. *Brain* 121: 2327–2334.
29. Sallusto, F., J. Geginat, and A. Lanzavecchia. 2004. Central memory and effector memory T cell subsets: function, generation, and maintenance. *Annu. Rev. Immunol.* 22: 745–763.
30. Toft-Hansen, H., R. Buist, X. J. Sun, A. Schellenberg, J. Peeling, and T. Owens. 2006. Metalloproteinases control brain inflammation induced by pertussis toxin in mice overexpressing the chemokine CCL2 in the central nervous system. *J. Immunol.* 177: 7242–7249.
31. Stüve, O., N. P. Dooley, J. H. Uhm, J. P. Antel, G. S. Francis, G. Williams, and V. W. Yong. 1996. Interferon beta-1b decreases the migration of T lymphocytes in vitro: effects on matrix metalloproteinase-9. *Ann. Neurol.* 40: 853–863.
32. Bar-Or, A., R. K. Nuttall, M. Duddy, A. Alter, H. J. Kim, I. Ifergan, C. J. Pennington, P. Bourgoin, D. R. Edwards, and V. W. Yong. 2003. Analyses of all matrix metalloproteinase members in leukocytes emphasize monocytes as major inflammatory mediators in multiple sclerosis. *Brain* 126: 2738–2749.
33. Chabas, D., S. E. Baranzini, D. Mitchell, C. C. Bernard, S. R. Rittling, D. T. Denhardt, R. A. Sobel, C. Lock, M. Karpuj, R. Pedotti, et al. 2001. The influence of the proinflammatory cytokine, osteopontin, on autoimmune demyelinating disease. *Science* 294: 1731–1735.
34. Shinohara, M. L., M. Jansson, E. S. Hwang, M. B. Werneck, L. H. Glimcher, and H. Cantor. 2005. T-bet-dependent expression of osteopontin contributes to T cell polarization. *Proc. Natl. Acad. Sci. USA* 102: 17101–17106.
35. Sixt, M., B. Engelhardt, F. Pausch, R. Hallmann, O. Wendler, and L. M. Sorokin. 2001. Endothelial cell laminin isoforms, laminins 8 and 10, play decisive roles in T cell recruitment across the blood-brain barrier in experimental autoimmune encephalomyelitis. *J. Cell Biol.* 153: 933–946.
36. Agrawal, S., P. Anderson, M. Durbeej, N. van Rooijen, F. Ivars, G. Opdenakker, and L. M. Sorokin. 2006. Dystroglycan is selectively cleaved at the parenchymal basement membrane at sites of leukocyte extravasation in experimental autoimmune encephalomyelitis. *J. Exp. Med.* 203: 1007–1019.
37. Moser, B., and P. Loetscher. 2001. Lymphocyte traffic control by chemokines. *Nat. Immunol.* 2: 123–128.
38. Sørensen, T. L., M. Tani, J. Jensen, V. Pierce, C. Lucchinetti, V. A. Folcik, S. Qin, J. Rottman, F. Sellebjerg, R. M. Strieter, et al. 1999. Expression of specific chemokines and chemokine receptors in the central nervous system of multiple sclerosis patients. *J. Clin. Invest.* 103: 807–815.
39. Kivisäkk, P., C. Trebst, Z. Liu, B. H. Tucky, T. L. Sørensen, R. A. Rudick, M. Mack, and R. M. Ransohoff. 2002. T-cells in the cerebrospinal fluid express a similar repertoire of inflammatory chemokine receptors in the absence or presence of CNS inflammation: implications for CNS trafficking. *Clin. Exp. Immunol.* 129: 510–518.
40. Balashov, K. E., J. B. Rottman, H. L. Weiner, and W. W. Hancock. 1999. CCR5(+) and CXCR3(+) T cells are increased in multiple sclerosis and their ligands MIP-1alpha and IP-10 are expressed in demyelinating brain lesions. *Proc. Natl. Acad. Sci. USA* 96: 6873–6878.
41. Franciotta, D., G. Martino, E. Zardini, R. Furlan, R. Bergamaschi, L. Andreoni, and V. Cosi. 2001. Serum and CSF levels of MCP-1 and IP-10 in multiple sclerosis patients with acute and stable disease and undergoing immunomodulatory therapies. *J. Neuroimmunol.* 115: 192–198.
42. Mahad, D., M. K. Callahan, K. A. Williams, E. E. Ubogu, P. Kivisäkk, B. Tucky, G. Kidd, G. A. Kingsbury, A. Chang, R. J. Fox, et al. 2006. Modulating CCR2 and CCL2 at the blood-brain barrier: relevance for multiple sclerosis pathogenesis. *Brain* 129: 212–223.
43. Subileau, E. A., P. Rezaie, H. A. Davies, F. M. Colyer, J. Greenwood, D. K. Male, and I. A. Romero. 2009. Expression of chemokines and their receptors by human brain endothelium: implications for multiple sclerosis. *J. Neuropathol. Exp. Neurol.* 68: 227–240.
44. dos Santos, A. C., M. M. Barsante, R. M. Arantes, C. C. Bernard, M. M. Teixeira, and J. Carvalho-Tavares. 2005. CCL2 and CCL5 mediate leukocyte adhesion in experimental autoimmune encephalomyelitis—an intravital microscopy study. *J. Neuroimmunol.* 162: 122–129.
45. Shulman, Z., S. J. Cohen, B. Roediger, V. Kalchenko, R. Jain, V. Grabovsky, E. Klein, V. Shinder, L. Stoler-Barak, S. W. Feigelson, et al. 2012. Transendothelial migration of lymphocytes mediated by intraendothelial vesicle stores rather than by extracellular chemokine depots. *Nat. Immunol.* 13: 67–76.
46. Denhardt, D. T., M. Noda, A. W. O'Regan, D. Pavlin, and J. S. Berman. 2001. Osteopontin as a means to cope with environmental insults: regulation of inflammation, tissue remodeling, and cell survival. *J. Clin. Invest.* 107: 1055–1061.
47. Zhang, H. H., K. Song, R. L. Rabin, B. J. Hill, S. P. Perfetto, M. Roederer, D. C. Douek, R. M. Siegel, and J. M. Farber. 2010. CCR2 identifies a stable population of human effector memory CD4+ T cells equipped for rapid recall response. *J. Immunol.* 185: 6646–6663.
48. Reboldi, A., C. Coisne, D. Baumjohann, F. Benvenuto, D. Bottinelli, S. Lira, A. Uccelli, A. Lanzavecchia, B. Engelhardt, and F. Sallusto. 2009. C-C chemokine receptor 6-regulated entry of TH-17 cells into the CNS through the choroid plexus is required for the initiation of EAE. *Nat. Immunol.* 10: 514–523.
49. Miller, D., F. Barkhof, X. Montalban, A. Thompson, and M. Filippi. 2005. Clinically isolated syndromes suggestive of multiple sclerosis, part I: natural history, pathogenesis, diagnosis, and prognosis. *Lancet Neurol.* 4: 281–288.
50. Weiner, H. L. 2008. A shift from adaptive to innate immunity: a potential mechanism of disease progression in multiple sclerosis. *J. Neurol.* 255(Suppl. 1): 3–11.

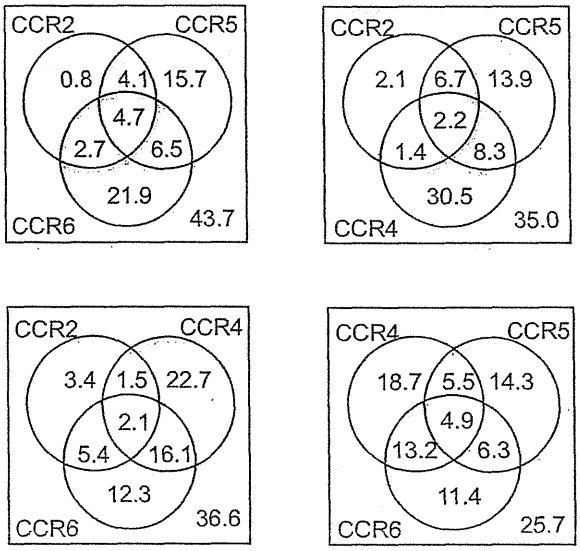

SUPPLEMENTAL FIGURE 1. Chemokine receptor expression profiles and its overlap in memory CD4$^+$ T cells from MS

For flow cytometric analysis, PBMC depleted of CD14$^+$ cells were stained with differentially labeled anti-CD4, -CD45RA, -CCR2, -CCR5, -CCR4 and -CCR6 mAbs simultaneously. Venn diagrams show frequencies (%) of the cells expressing CCR2, CCR4, CCR5 and CCR6 in memory CD4$^+$ T cells in PB from 11 MS patients in remission. The combination of 3 chemokine receptors out of 4 is shown in each panel.

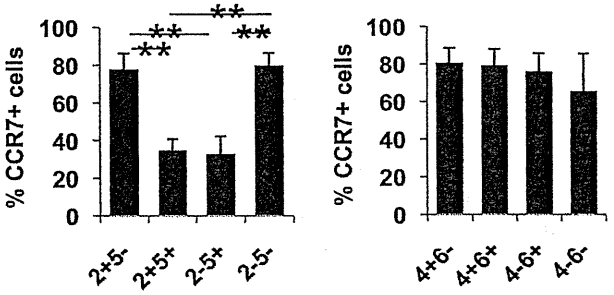

SUPPLEMENTAL FIGURE 2. Frequency of CCR7 expression in memory CD4$^+$ T cell subsets defined by chemokine receptor expression profile
Shown are the proportions of CCR7$^+$ cells within each memory CD4$^+$ T cell subset defined by expression of CCR2 and CCR5 (left), and of CCR4 and CCR6 (right).

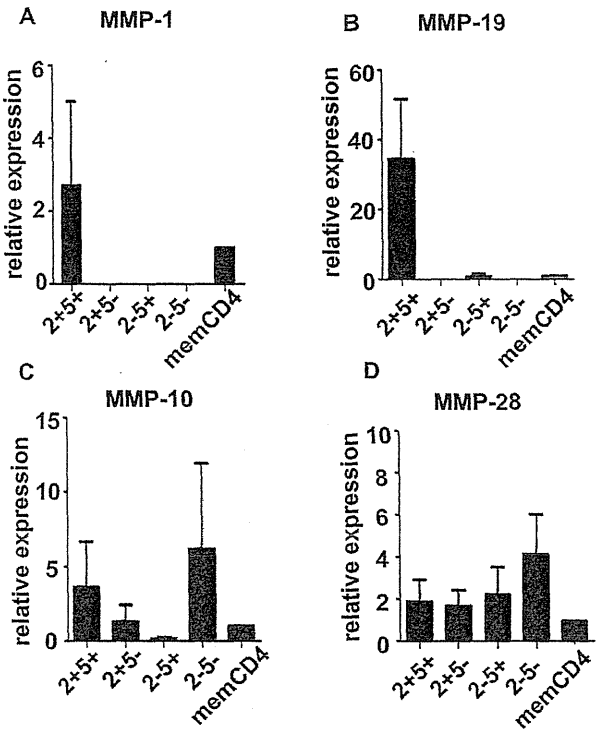

SUPPLEMENTAL FIGURE 3. Expression levels of MMP-1, -19, -10, and -28 in memory CD4$^+$ T cells
Each memory CD4$^+$ T cell subset was purified from the PB of HS individuals and was stimulated with PMA and ionomycin. The expression levels of the MMP mRNAs were determined by quantitative RT-PCR. Data represent mean values ± SD of 4 different subjects.

Supplemental Table. Frequencies of memory CD4$^+$ T cell subsets determined by chemokine receptor expression

	HS (%)	MS (%)
2+5+4+6−	0.69±0.46	1.05±0.59
2+5+4+6+	0.88±0.87	1.09±0.78
2+5+4−6+	2.91±2.47	3.6±1.72
2+5+4−6−	3.05±1.91	3.08±1.05
2+5−4+6−	0.27±0.24	0.4±0.37
2+5−4+6+	0.57±0.49	0.95±0.79
2+5−4−6+	1.35±1.35	1.78±1.21
2+5−4−6−	0.46±0.25	0.36±0.19
2−5+4+6−	3.49±1.52	4.43±1.82
2−5+4+6+	3.63±1.95	3.84±1.39
2−5+4−6+	2.19±0.92	2.67±1.22
2−5+4−6−	9.38±4.61	11.26±6.79
2−5−4+6−	18.72±5.07	18.32±5.01
2−5−4+6+	11.91±3.91	12.21±3.34
2−5−4−6+	9.04±3.10	9.62±1.53
2−5−4−6−	31.49±8.55	25.33±4.83

Memory CD4+ T cells were divided into 16 subsets based on the expression of CCR2, CCR5, CCR4, and CCR6. Data from 11 HS and 11 patients with MS in remission were analyzed.

INTERNAL MEDICINE

CASE REPORT

New-Onset Type 1 Diabetes Mellitus and Anti-Aquaporin-4 Antibody Positive Optic Neuritis Associated with Type 1 Interferon Therapy for Chronic Hepatitis C

Tomoya Kawazoe[1], Manabu Araki[1], Youwei Lin[1], Masafumi Ogawa[1], Tomoko Okamoto[1], Takashi Yamamura[2], Masato Wakakura[3] and Miho Murata[1]

Abstract

A 60-year-old woman developed type 1 diabetes mellitus and anti-aquaporin-4 antibody positive optic neuritis during type 1 interferon therapies for chronic hepatitis C. The diabetes mellitus was elicited by interferon-α plus ribavirin therapy, while the optic neuritis was induced after interferon-β treatment, followed by interferon-α and ribavirin therapy. It is possible that type 1 interferons lead to the onset of the two autoimmune diseases by inducing disease-specific autoantibodies. Autoimmune disease is an infrequent complication of type 1 interferon treatment; however, once it has occurred, it may result in severe impairments. Patients undergoing type 1 interferon therapy should therefore be carefully monitored for any manifestations of autoimmune diseases.

Key words: aquaporin-4, neuromyelitis optica, chronic hepatitis C, type 1 diabetes mellitus, type 1 interferon

(Intern Med 51: 2625-2629, 2012)
(DOI: 10.2169/internalmedicine.51.7771)

Introduction

Type 1 interferon (IFN) is widely used to treat patients with chronic viral hepatitis and malignant neoplasms. Approximately two million people in Japan are infected with the hepatitis C virus (HCV). Combination therapy with type 1 IFN and ribavirin (RBV) is used in 50,000-100,000 patients annually. Since type 1 IFN has not only antiviral and antiproliferative effects, but also immunomodulatory effects, it can occasionally induce various autoimmune diseases (1). The onset of autoimmune diseases can be attributed to the overproduction of disease-specific antibodies. We herein present the case of a patient who developed type 1 diabetes mellitus (T1DM) and severe optic neuritis with anti-aquaporin-4 (AQP-4) antibodies during treatment with combinations including IFN-α and IFN-β for chronic hepatitis C.

Case Report

A 60-year-old Japanese woman was diagnosed with hepatitis C (type 1b) in 1994 at the age of 42 years. Since the diagnosis, she had received various types of IFN therapy: natural IFN-α, recombinant IFN-α-2b and RBV, recombinant IFN-αcon-1, and pegylated IFN (PEG-IFN)-α-2b and RBV (Fig. 1). From 1994 to 2008, all of the above-mentioned IFN therapies resulted in a transient reduction in HCV-RNA to undetectable levels, but a sustained virologic response (SVR) was not obtained. While undergoing PEG-IFN/RBV treatment, the patient was noted to have hyperglycemia, and she was diagnosed with T1DM in 2008 (Fig. 1). She was found to be positive for anti-glutamic acid decarboxylase (GAD) antibodies, with a titer of 3,440x. The titers of anti-GAD antibodies were decreased to 128x two years after the initiation of insulin treatment.

In January 2009, the patient underwent combination therapy for virus eradication by double-filtration plasmapheresis

[1]Department of Neurology, National Center Hospital, National Center of Neurology and Psychiatry, Japan, [2]Department of Immunology, National Institute of Neuroscience, National Center of Neurology and Psychiatry, Japan and [3]Inouye Eye Hospital, Japan
Received for publication May 24, 2012; Accepted for publication June 25, 2012
Correspondence to Dr. Manabu Araki, m-araki@ncnp.go.jp

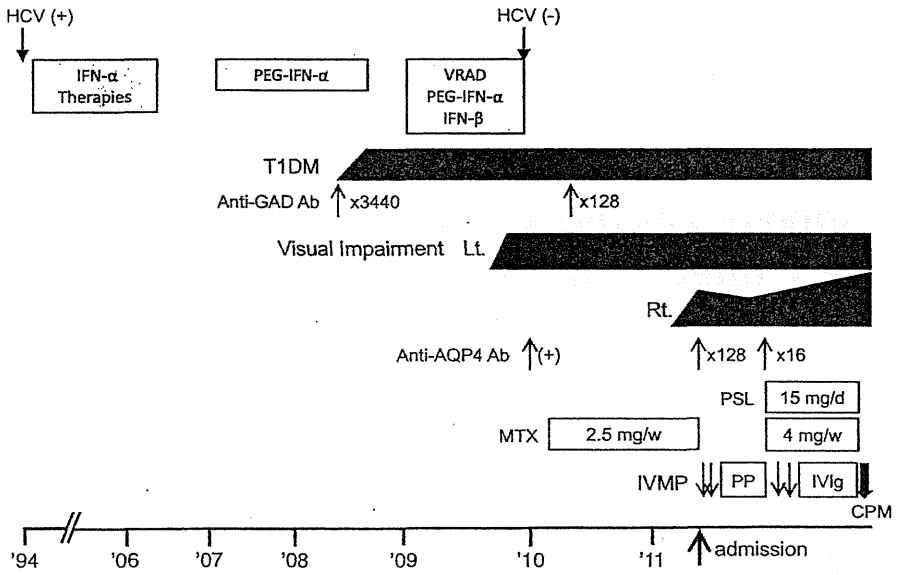

Figure 1. The clinical course of the present case. Anti-AQP-4 Ab: anti-aquaporin-4 antibody, Anti-GAD antibody: Anti-glutamic acid decarboxylase antibody, CPM: cyclophosphamide, HCV: hepatitis C virus, IFN-a therapies: IFN-α for 24 weeks from 1994 to 1995, IFN-α-2b/Ribavirin (RBV) for 24 weeks in 2002, IFN-αcon-1 for 12 weeks in 2004, and PEG-IFN-α-2b/RBV for 48 weeks from 2005 to 2006, IVIg: intravenous immunoglobulin, IVMP: intravenous methylprednisolone, MTX: methotrexate, PEG-IFN: pegylated IFN-α-2b and RBV, PP: plasmapheresis, PSL: prednisolone, T1DM: type 1 diabetes mellitus, VRAD: virus removal and eradication by double-filtration plasmapheresis (DFPP)

(VRAD), intravenous natural IFN-β for 14 days, and PEG-IFN-α-2a plus RBV for 36 weeks to achieve HCV-RNA seronegativity. A SVR was finally achieved with these intensive combination therapies (Fig. 1).

In November 2009, the patient experienced pain when moving her left eye. Her left visual acuity deteriorated to light perception within two weeks. She was diagnosed with left optic neuritis. The IFN therapy was terminated, and triamcinolone was injected locally into the subtenon of the affected side, which was not effective. Serological tests demonstrated that she was positive for AQP-4 antibodies in January 2010, and hence a clinical diagnosis of neuromyelitis optica spectrum disorder (NMOsd) was made (Fig. 1).

To prevent relapse and progression of the optic neuritis, immunosuppressant drug therapy was initiated, with weekly oral methotrexate (MTX) administration at a dose of 2.5 mg. In June 2011, right optic neuritis occurred and the right visual acuity was decreased from normal to finger counting within two weeks. She received two courses of high-dose intravenous methylprednisolone (IVMP) therapy, which were not effective. She was admitted to our hospital for further treatment (Fig. 1).

On admission, her neurological findings were normal, except for the severe visual impairment of 0.02 (20/1,000) in both eyes. The visual field defects were detected by Goldmann perimetry (Fig. 2A). Ophthalmoscopy showed no impairment of the retinal blood vessels. The visual evoked potential indicated no response. The cerebrospinal fluid was normal, with a cell count of less than 1/μL with all mononuclear cells, and a protein concentration of 37 mg/dL. Oligoclonal banding was negative, and the myelin basic protein level was within the normal range. The serum blood sugar level was 196 mg/dL (normal range 70-110), glycosylated hemoglobin was 6.7% (normal range 4.3-5.8), and the anti-GAD antibodies were detected with a value of 9.9 U/mL. The patient's serum was also found to be positive for anti-AQP-4 antibodies, with a titer of 128x. Anti-nuclear antibodies, anti-SS-A/SS-B antibodies, anti-neutrophil cytoplasmic antibodies, and anti-thyroid antibodies were not detected.

Magnetic resonance imaging (MRI) showed a high signal intensity of the left optic nerve on T2-weighted and fluid-attenuated inversion recovery, and T1-weighted imaging with contrast enhancement, whereas the right optic nerve showed no particular findings (Fig. 2B, C). Brain MRI (Fig. 2D, E) showed a small number of high-intensity spots in the cerebral white matter. No obvious abnormality was observed in the spinal cord MRI.

The patient was treated with eight courses of plasmapheresis. During the treatment, her visual acuity slightly improved and she could read a few written characters. The titer of the anti-AQP-4 antibodies was decreased to 16x. However, the patient's visual field defect gradually worsened again soon after the discontinuation of plasmapheresis, so we initiated two courses of IVMP therapy, an additional two courses of plasmapheresis, high-dose intravenous immu-

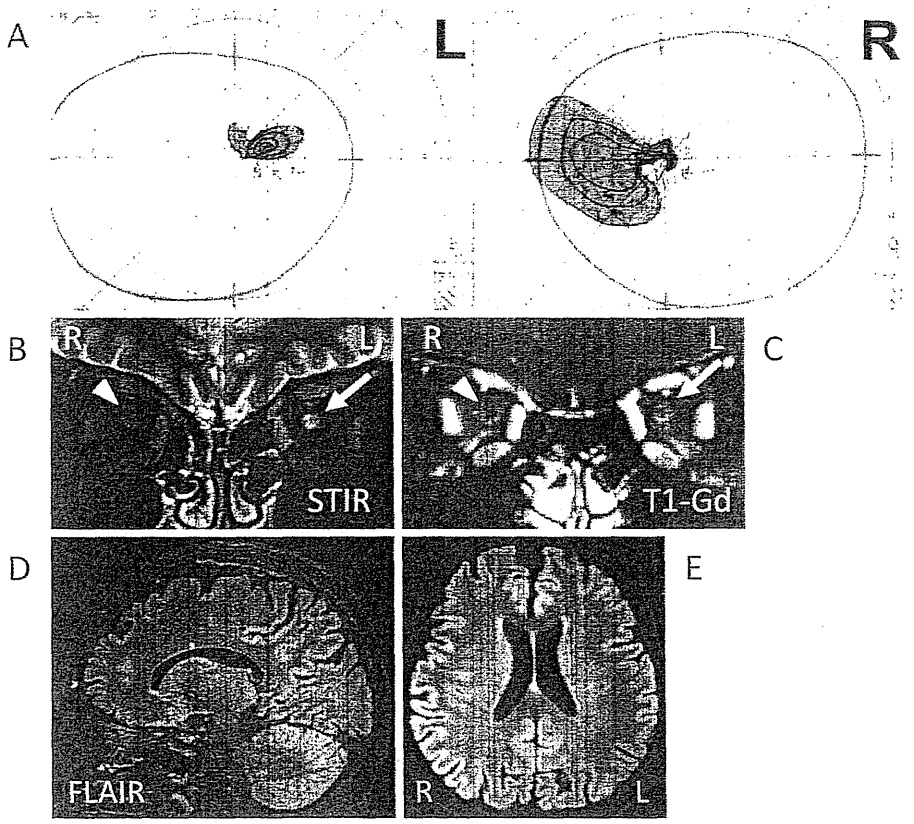

Figure 2. **The visual impairment and the magnetic resonance images of the present case. The Goldmann visual fields on admission are highlighted (A). The left optic nerve showed high signal intensity on the STIR coronal image (white arrow, B) with marginal contrast enhancement (white arrow, C). The right optic nerve showed no remarkable findings (arrow head, B and C). The brain showed no particular findings except for the optic nerve on FLAIR saggital (D) and axial (E) images. FLAIR: fluid-attenuated inversion recovery, STIR: short inversion time inversion-recovery, T1-Gd: gadolinium enhanced T1**

noglobulin (400 mg/kg/day for five days), and high-dose cyclophosphamide (CPM) (500 mg/day for one day). The exacerbation of the visual impairment was halted by this treatment. In September 2011, the patient was discharged from our hospital with a plan to undergo monthly CPM therapy.

Discussion

The present patient developed T1DM during IFN-α therapy and anti-AQP4 antibody positive optic neuritis after IFN-β, followed by IFN-α, therapy. Her severe visual impairment persisted despite the use of intensive immunotherapy. Several reasons for the intractable disease course can be proposed. For example, the type 1 IFNs or HCV infection may have served as a potent activator of autoimmunity, or the involvement of vasculitis as an extrahepatic manifestation of HCV infection (2) could lead to the clinical deterioration.

The first case of T1DM development during IFN-α therapy for chronic hepatitis C was reported in 1992 (3). New-onset DM among IFN-treated patients has been documented to occur in 0.7% of patients in Japan (4). The mechanism underlying immune-mediated pancreatic β-cell destruction can be attributed to genetic and environmental causes thus leading to the generation of islet cell autoantibodies, i.e., anti-GAD autoantibodies. IFN-α may act as an initiator of the autoimmunity directed against β cells, thus leading to the pathogenesis of T1DM. Likewise, IFN-α can be considered to play a critical role in the pathogenesis of systemic lupus erythematosus.

To date, ten cases of new-onset optic neuritis, multiple sclerosis (MS), MS-like disease, or NMOsd associated with IFN-α therapy for chronic viral hepatitis or malignant neoplasms, have been reported (5-11). There were two cases with seropositivity for anti-AQP4 antibodies (Table); one patient with optic-spinal MS (OSMS) after IFN-α2b and RBV (10), and another patient with NMOsd after PEG-IFN-α and RBV (11). In the remaining eight cases, the presence of anti-AQP-4 antibodies was not examined because they had been reported before the discovery of NMO-Immunoglobulin G (IgG) and anti-AQP-4 (12) antibodies.

IFN-β therapy can also play a role as an initiator of autoimmune diseases involving the central nervous system. A case with new-onset optic neuritis after IFN-β therapy for

Table. The Reported Cases of Newly-onset Anti-AQP-4 Antibody Positive OSMS, and NMOsd Provoked by Type 1 IFN Therapy

Patient age, sex	Disease	IFN	ON	SC	B	AQP4-Ab	Duration	References
47, F	Hepatitis C	α-2b/RBV	+	+	+	+	1Y	Kajiyama, et al. 2007[10]
65, F	Hepatitis C	α/RBV	+	-	+	+	2Y10M	Yamasaki, et al. 2012[11]
60, F	Hepatitis C	α, β, α/RBV	+	-	-	+	α: 15Y β: 9M	Present Case 2012

RBV: ribavirin, ON: optic neuritis, SC: spinal cord lesion, B: brain lesion. Duration: duration between the initiation of type 1 IFN therapy and the onset of OSMS or NMOsd

kidney cancer has been reported (13). In addition, a number of exacerbated cases of relapsing-remitting MS (RRMS) have been reported in Japan in patients receiving IFN-β (14). Differentiating between NMO and MS can be achieved based on seropositivity for the anti-AQP-4 antibodies, longitudinally extensive spinal cord lesions, and brain MRI findings not meeting the diagnostic criteria for MS (15). However, before the discovery of this autoantibody, it was difficult to distinguish NMO from MS, especially OSMS, which is common in Asian countries. In 2000, IFN-β therapy was approved in Japan for the prevention of relapse and progression of RRMS, in which patients with OSMS were also included. Consequently, exacerbation of the disease or ineffectiveness of IFN-β was reported among patients with OSMS who underwent IFN-β therapy (14, 16). These cases were later found to be positive for anti-AQP-4 antibodies. Recent articles described that IFN-β treatment was not effective in preventing relapses in NMO patients (17, 18), while strictly defined OSMS showed a response to IFN-β treatment in terms of the prevention of relapses and functional worsening (19).

The mechanism underlying the onset and exacerbation of NMO/NMOsd has not been well understood, but the induction of B-cell activation factors of the tumor necrosis factor (TNF) family by IFN-β is considered to facilitate the production of anti-AQP-4 antibodies (20). For example, Chihara et al. have shown that IL-6-dependent B-cell subpopulations of plasmablasts are involved in the production of anti-AQP-4 antibodies (21). Loss of AQP-4, mediated by immunoglobulins and complements, has been shown in inflammatory lesions of patients with NMO (22). These results indicate that the anti-AQP-4 antibody plays a crucial role in the pathogenesis of NMO, unlike in cases of MS. As another mechanism underlying the development of type 1 IFN-induced NMO/NMOsd, it has been suggested that IFN-β treatment leads to the overproduction of IL-17 from T helper 17 (Th17) cells (23), which is thought to be associated with the pathological feature of NMO.

Type 1 IFN has reciprocal characteristics, with both pathogenic and protective roles in autoimmunity. In general, IFN-β exerts its therapeutic effect on MS by producing anti-inflammatory cytokines and suppressing the proliferation of autoreactive T cells. Both IFN-α and IFN-β bind to a single heterodimeric receptor composed of IFNAR1 and IFNAR2, which can cause similar immunomodulatory effects (24). Hence, it is likely that IFN-α has a similar effect on autoimmunity as does IFN-β, as indicated by the fact that IFN-α has also been developed as a candidate therapeutic agent for MS (25).

Type 1 IFNs served as pathogenic mediators in the present case, inducing T1DM and NMO/NMOsd. Since various types of IFN-α treatment had been carried out intermittently for more than ten years after the onset of chronic hepatitis C, the onset of T1DM was clearly influenced by IFN-α treatment. However, it remains unclear which type of IFN was involved in the induction of NMOsd. We speculate that the combination therapy with IFN-α and IFN-β may have produced synergistic effects to trigger NMOsd in the present case.

The authors state that they have no Conflict of Interest (COI).

Acknowledgement

We thank Dr. Toshiyuki Takahashi from the Department of Neurology and Multiple Sclerosis Therapeutics, Tohoku University Graduate School of Medicine, for measuring the titer of anti-AQP-4 antibodies. We also thank Dr. Motoki Takashima and Dr. Akihisa Miyazaki from the Department of Gastroenterology, Juntendo University Nerima Hospital, for providing the medical information on hepatitis C.

Contributor TK, MA, and MW undertook the clinical management of the patient. MW referred the patient to NCNP and performed the ophthalmological examination. Each of the authors was significantly involved in clinical assessments of the patient. TK and MA equally contributed to this work.

References

1. Burdick LM, Somani N, Somani AK. Type I IFNs and their role in the development of autoimmune diseases. Expert Opin Drug Saf 8: 459-472, 2009.
2. Cacoub P, Poynard T, Ghillani P, et al. Extrahepatic manifestations of chronic hepatitis C. Arthritis Rheum 42: 2204-2212, 1999.
3. Fabris P, Betterle C, Floreani A, et al. Development of type 1 dia-

betes mellitus during interferon alfa therapy for chronic HCV hepatitis. Lancet **340**: 548, 1992.
4. Okanoue T, Sakamoto S, Itoh Y, et al. Side effects of high-dose interferon therapy for chronic hepatitis C. J Hepatol **25**: 283-291, 1996.
5. Manesis EK, Petrou C, Brouzas D, Hadziyannis S. Optic tract neuropathy complicating low-dose interferon treatment. J Hepatol **21**: 474-477, 1994.
6. Isler M, Akhan G, Bardak Y, Akkaya A. Dry cough and optic neuritis: two rare complications of interferon alpha treatment in chronic viral hepatitis. Am J Gastroenterol **96**: 1303-1304, 2001.
7. Matsuo T, Takabatake R. Multiple sclerosis-like disease secondary to alpha interferon. Ocul Immunol Inflamm **10**: 299-304, 2002.
8. Kataoka I, Shinagawa K, Shiro Y, et al. Multiple sclerosis associated with interferon-alpha therapy for chronic myelogenous leukemia. Am J Hematol **70**: 149-153, 2002.
9. Höftberger R, Garzuly F, Dienes HP, et al. Fulminant central nervous system demyelination associated with interferon-alpha therapy and hepatitis C virus infection. Mult Scler **13**: 1100-1106, 2007.
10. Kajiyama K, Tsuda K, Takeda M, Yoshikawa H, Tanaka K. Multiple sclerosis with positive anti-aquaporin-4 antibody, manifested after interferon-a-2b/ribavirin therapy for chronic hepatitis C. A case report. Shinkeinaika (Neurol Med) **66**: 180-184, 2007 (in Japanese, Abstract in English).
11. Yamasaki M, Matsumoto K, Takahashi Y, Nakanishi H, Kawai Y, Miyamura M. A case of NMO (Neuromyelitis optica) spectrum disorder triggered by interferon alpha, which involved extensively pyramidal tract lesion of the brain. Rinshou Shinkeigaku (Clin Neurol) **52**: 19-24, 2012.
12. Lennon VA, Wingerchuk DM, Kryzer TJ, et al. A serum autoantibody marker of neuromyelitis optica: distinction from multiple sclerosis. Lancet **364**: 2106-2112, 2004.
13. Okuma H, Kawamura Y, Ohnuki Y, Takagi S. Optic neuritis caused by interferon-beta administration. Intern Med **47**: 1759, 2008.
14. Shimizu J, Hatanaka Y, Hasegawa M, et al. IFNβ-1b may severely exacerbate Japanese optic-spinal MS in neuromyelitis optica spectrum. Neurology **75**: 1423-1427, 2010.
15. Wingerchuk DM, Lennon VA, Pittock SJ, Lucchinetti CF, Weinshenker BG. Revised diagnostic criteria for neuromyelitis optica. Neurology **66**: 1485-1489, 2006.
16. Matsuoka T, Matsushita T, Kawano Y, et al. Heterogeneity of aquaporin-4 autoimmunity and spinal cord lesions in multiple sclerosis in Japanese. Brain **130**: 1206-1223, 2007.
17. Tanaka M, Tanaka K, Komori M. Interferon-beta(1b) treatment in neuromyelitis optica. Eur Neurol **62**: 167-170, 2009.
18. Uzawa A, Mori M, Hayakawa S, Masuda S, Kuwabara S. Different responses to interferon beta-1b treatment in patients with neuromyelitis optica and multiple sclerosis. Eur J Neurol **17**: 672-676, 2010.
19. Shimizu Y, Fujihara K, Kubo S, et al. Therapeutic efficacy of interferon b-1b in Japanese patients with optic-spinal multiple sclerosis. Tohoku J Exp Med **223**: 211-214, 2011.
20. Krumbholz M, Faber H, Steinmeyer F, et al. Interferon-beta increases BAFF levels in multiple sclerosis: implications for B cell autoimmunity. Brain **131**: 1455-1463, 2008.
21. Chihara N, Aranami T, Sato W, et al. Interleukin 6 signaling promotes anti-aquaporin 4 autoantibody production from plasmablasts in neuromyelitis optica. Proc Natl Acad Sci U S A **108**: 3701-3706, 2011.
22. Misu T, Fujihara K, Kakita A, et al. Loss of aquaporin 4 in lesions of neuromyelitis optica: distinction from multiple sclerosis. Brain **130**: 1224-1234, 2007.
23. Axtell RC, Raman C, Steinman L. Interferon-b exacerbates Th17-mediated inflammatory disease. Trends Immunol **32**: 272-277, 2011.
24. Crow MK. Type 1 interferon in organ-targeted autoimmune and inflammatory diseases. Arthritis Res Ther **12**(Suppl 1): S5-S14, 2010.
25. Knobler RL, Panitch HS, Braheny SL, et al. Systemic alpha-interferon therapy of multiple sclerosis. Neurology **34**: 1273-1279, 1984.

ARTICLE IN PRESS

JNS-12224; No of Pages 6

Journal of the Neurological Sciences xxx (2012) xxx–xxx

Contents lists available at SciVerse ScienceDirect

Journal of the Neurological Sciences

journal homepage: www.elsevier.com/locate/jns

Heterozygous UDP-GlcNAc 2-epimerase and *N*-acetylmannosamine kinase domain mutations in the *GNE* gene result in a less severe GNE myopathy phenotype compared to homozygous *N*-acetylmannosamine kinase domain mutations

Madoka Mori-Yoshimura [a,*], Kazunari Monma [b], Naoki Suzuki [c], Masashi Aoki [c], Toshihide Kumamoto [d], Keiko Tanaka [e], Hiroyuki Tomimitsu [f], Satoshi Nakano [g], Masahiro Sonoo [h], Jun Shimizu [i], Kazuma Sugie [j], Harumasa Nakamura [a,k], Yasushi Oya [a], Yukiko K. Hayashi [b], May Christine V. Malicdan [b], Satoru Noguchi [b], Miho Murata [a], Ichizo Nishino [b]

[a] *Department of Neurology, National Center Hospital, National Center of Neurology and Psychiatry, 4-1-1 Ogawahigashi, Kodaira, Tokyo 187-8551, Japan*
[b] *Department of Neuromuscular Research, National Institute of Neuroscience, National Center of Neurology and Psychiatry, 4-1-1 Ogawahigashi, Kodaira, Tokyo 187-8502, Japan*
[c] *Department of Neurology, Tohoku University School of Medicine, 1-1 Seiryo, Aoba-ku, Sendai 980-8574, Japan*
[d] *Department of Internal Medicine 3, Faculty of Medicine, Oita University, 1-1 Idaigaoka, Hasama, Yufu-shi, Oita 879-5593, Japan*
[e] *Department of Neurology, Kanazawa Medical University, 1-1 Daigaku, Uchinadamachi, Kahoku-gun, Ishikawa, 920-0214, Japan*
[f] *Department of Neurology and Neurological Science, Graduate School, Tokyo Medical and Dental University, Yushima 1-5-45, Bunkyo-ku, Tokyo 113-8519, Japan*
[g] *Department of Neurology, Osaka City General Hospital, 2-13-22, Miyakojimahonndoori, Miyakojima-ku, Osaka534-0021, Japan*
[h] *Department of Neurology, Teikyo University School of Medicine, Kaga 2-11-1, Itabashi-ku, Tokyo 173-8605, Japan*
[i] *Department of Neurology, Division of Neuroscience, Graduate School of Medicine, University of Tokyo, 7-3-1 Hongo, Bunkyo-ku, Tokyo 113-8655, Japan*
[j] *Department of Neurology, Nara Medical University School of Medicine, 840 Shijo, Kashihara, Nara 634-8521, Japan*
[k] *Clinical Trial Division, Division of Clinical Research, National Center Hospital of Neurology and Psychiatry, 4-1-1 Ogawahigashi, Kodaira, Tokyo 187-8551, Japan*

ARTICLE INFO

Article history:
Received 10 January 2012
Received in revised form 20 March 2012
Accepted 21 March 2012
Available online xxxx

Keywords:
GNE myopathy
Distal myopathy with rimmed vacuoles
Hereditary inclusion body myopathy
Glucosamine (UDP-N-acetyl)-2-epimerase/*N*-acetylmannosamine kinase
(UDP-N-acetyl)-2-epimerase domain
N-acetylmannosamine kinase domain
Questionnaire
Natural history

ABSTRACT

Background: Glucosamine (UDP-N-acetyl)-2-epimerase/*N*-acetylmannosamine kinase (GNE) myopathy, also called distal myopathy with rimmed vacuoles (DMRV) or hereditary inclusion body myopathy (HIBM), is a rare, progressive autosomal recessive disorder caused by mutations in the *GNE* gene. Here, we examined the relationship between genotype and clinical phenotype in participants with GNE myopathy.
Methods: Participants with GNE myopathy were asked to complete a questionnaire regarding medical history and current symptoms.
Results: A total of 71 participants with genetically confirmed GNE myopathy (27 males and 44 females; mean age, 43.1 ± 13.0 (mean ± SD) years) completed the questionnaire. Initial symptoms (*e.g.*, foot drop and lower limb weakness) appeared at a mean age of 24.8 ± 8.3 years. Among the 71 participants, 11 (15.5%) had the ability to walk, with a median time to loss of ambulation of 17.0 ± 2.1 years after disease onset. Participants with a homozygous mutation (p.V572L) in the *N*-acetylmannosamine kinase domain (KD/KD participants) had an earlier disease onset compared to compound heterozygous participants with mutations in the uridine diphosphate-N-acetylglucosamine (UDP-GlcNAc) 2-epimerase and *N*-acetylmannosamine kinase domains (ED/KD participants; 26.3 ± 7.3 vs. 21.2 ± 11.1 years, respectively). KD/KD participants were more frequently non-ambulatory compared to ED/KD participants at the time of survey (80% vs. 50%). Data were verified using medical records available from 17 outpatient participants.
Conclusions: Homozygous KD/KD participants exhibited a more severe phenotype compared to heterozygous ED/KD participants.

1. Introduction

Glucosamine (UDP-N-acetyl)-2-epimerase/*N*-acetylmannosamine kinase (GNE) myopathy, also known as distal myopathy with rimmed vacuoles (DMRV), Nonaka myopathy (MIM: 605820) or hereditary inclusion body myopathy (HIBM; MIM: 600737), is an early adult-onset, progressive myopathy that affects the tibialis anterior muscle, but spares quadriceps femoris muscles [1,2]. The disease is caused by a mutation in the *GNE* gene, which encodes a bifunctional enzyme [uridine diphosphate-*N*-acetylglucosamine (UDP-GlcNAc) 2-epimerase (GNE) and *N*-acetylmannosamine kinase (MNK)] known to catalyze two rate-limiting reactions involved in cytosolic sialic acid synthesis [3–7]. Mutations in the *GNE* gene result in decreased enzymatic activity *in vitro* by 30–90% [7–10]. Therefore, hyposialylation is thought to

* Corresponding author. Tel.: +81 42 341 2711; fax: +81 42 346 1852.
E-mail address: yoshimur@ncnp.go.jp (M. Mori-Yoshimura).

0022-510X/$ – see front matter © 2012 Elsevier B.V. All rights reserved.
doi:10.1016/j.jns.2012.03.016

Please cite this article as: Mori-Yoshimura M, et al, Heterozygous UDP-GlcNAc 2-epimerase and *N*-acetylmannosamine kinase domain mutations in the *GNE*..., J Neurol Sci (2012), doi:10.1016/j.jns.2012.03.016

contribute to the pathogenesis of GNE myopathy. This is supported by the myopathic phenotype associated with a mouse model expressing the human D176V mutant GNE protein (GNE−/−hGNED176V-Tg) [11]. Muscle atrophy and weakness are prevented by oral treatment with sialic acid metabolites in this mouse model [12].

A phase I clinical trial using oral sialic acid therapy has recently been performed in Japan for the treatment of GNE myopathy (ClinicalTrials.gov; NCT01236898). A similar phase I study is currently underway in the United States (ClinicalTrials.gov; NCT01359319). Natural history and genotype–phenotype correlations need to be established for a successful phase II clinical trial for the treatment of GNE myopathy. However, only a small number of studies have been conducted that review the natural course of this disease. In addition, the presence of genotype–phenotype correlations is controversial in GNE myopathy, with most reports denying significant correlations [7]. In fact, substantial heterogeneity is observed among participants who have the same mutations. For example, few subjects with p.D176V and p.M712T mutations exhibited a normal or very mild phenotype, with disease onset after the age of 60 [3,13]. Furthermore, only a limited number of studies that analyze compound heterozygous patients are available. Nonetheless, such studies report a variable degree of severity [14–17].

To clarify the potential relationship between genotype and clinical phenotype (*i.e.*, age at onset, disease course, and current symptoms) of GNE myopathy, we performed a questionnaire-based survey of participants with confirmed GNE myopathy.

2. Participants and methods

2.1. Study population

We obtained approval for this study from the Medical Ethics Committee of the National Center of Neurology and Psychiatry (NCNP). Seventy-eight participants with known GNE myopathy were seen at 8 hospitals specializing in muscle disorders in Japan and 83 participants (not all genetically diagnosed) from the Participants Association for Distal Myopathies (PADM) were recruited. Participants provided written informed consent prior to completing the questionnaire.

A total of 75 participants completed and returned the questionnaire. Of the 75 participants analyzed, 4 were found to have only one heterozygous mutation. Because single heterozygous mutations have not been confirmed to cause GNE myopathy, these 4 participants were excluded from this study.

2.2. Study design

The present study is a retrospective and cross-sectional analysis, which includes 71 participants with genetically confirmed GNE myopathy. Clinical information was collected from participants using a questionnaire and genetic information was acquired from available medical records.

2.3. Questionnaire

Participants completed a self-reporting questionnaire regarding 1) developmental and past symptoms, 2) past and present ambulatory status, and 3) information about diagnosis and medical services (Supplementary material, original version in Japanese).

To determine developmental history, we collected the following information: 1) trouble before and/or during delivery, 2) body weight and height at birth, 3) age at first gait, 4) exercise performance during nursery, kindergarten, or school, and 5) age at onset and signs of first symptoms. Participants were also asked about the onset of 1) gait disturbance, 2) walking with assistance (*i.e.*, cane and/or orthotics and/or handrails), 3) wheelchair use, 4) loss of ambulation, and 5) current gait performance. With regard to medical history, participants were asked about 1) age at the time of first hospital visit, 2) whether or not they had symptoms at the time of visit, 3) age at the time of final diagnosis, 4) how many hospitals/clinics were visited before final diagnosis, and 5) whether a biopsy was performed.

2.4. Medical record examination

To verify the accuracy of the information provided by each participant, available medical records from 17 participants (23.9%) seen at outpatient clinics at NCNP were examined (9 males and 8 females).

2.5. Data handling and analysis

All variables were summarized using descriptive statistics, which included mean, standard deviation (SD), median, range, frequency, and percentage. Each variable was compared against age, sex, genotype, and domain mutation (*i.e.*, within the UDP-GlcNAc 2-epimerase domain: ED or *N*-acetylmannosamine kinase domain: KD). Student's *t* test was used to compare the means for each participant group (ED/ED, ED/KD and KD/KD participants). Data from the two participant groups were calculated using chi-square contingency table analysis. The time from disease onset to walking with assistance, time from disease onset to wheelchair use, and time from disease onset to loss of ambulation were evaluated using the Kaplan–Meier method with log-rank analysis. Questionnaire reliability was tested using intraclass correlation coefficients (ICCs), and two-sided 95% confidence intervals (CIs) were calculated using a one-way random effects analysis of variance model for inter-rater reliability. All analyses were performed using SPSS for Macintosh (version 18, SPSS Inc., Chicago, IL).

3. Results

3.1. General characteristics

A total of 71 Japanese individuals (27 males and 44 females) participated in the study. The mean age at data collection was 43.1 ± 10.7 years. None of the participants showed developmental abnormalities during infancy or early childhood.

3.2. GNE mutations

Forty-one percent of study participants (n = 29/71) had homozygous mutations, while 59% (n = 42/71) had compound heterozygous mutations (Table 1). Among homozygous participants, 86.2% (n = 25/29) harbored the p.V572L mutation, while the remaining participants had other mutations. No homozygous participants for the p.D176V mutation were identified. Among compound heterozygous participants, 28.5% (n = 12/42) had p.D176V/p.V572L mutations, while the remaining participants had other mutations. With respect to allelic frequency, 50.0% (71/142) were p.V572L, 20.4% (29/142) p.D176V, 3.5% (5/142) p.C13S, 2.8% (4/142) p.M712T, and 2.1% (3/142) p.A630T. All other mutations accounted for 2%. A total of 18.3% (n = 13/71) of participants were homozygous with a mutation in the GNE domain (ED/ED), 39.4% (n = 28/71) of participants were compound heterozygous with a mutation in the GNE domain and one in the MNK domain (ED/KD), and 42.3% (n = 30/71) of participants had a mutation in the MNK domain in both alleles (KD/KD).

3.3. Past and present symptoms

Mean participant age at symptom onset was 25.2 ± 9.2 years (range, 12–58 years; median, 24.5 years). There was no significant difference between males and females for current age, age at disease

Please cite this article as: Mori-Yoshimura M, et al, Heterozygous UDP-GlcNAc 2-epimerase and *N*-acetylmannosamine kinase domain mutations in the *GNE*..., J Neurol Sci (2012), doi:10.1016/j.jns.2012.03.016

Table 1
Genotypes of the GNE myopathy patient population.

		Questionnaire	Outpatients
ED/ED	Total	13	4
	Homozygote	1	0
	p.C13S homozygote	1	
	Compound heterozygote	12	4
	p.C13S/p.M29T	1	1
	p.C13S/p.A63I	1	1
	p.D176V/p.F233S	1	1
	p.D176V/p.R306Q	2	
	p.R129Q/p.D176V	1	
	p.R129Q/p.R277C	1	
	p.D27L/p.D176V	1	1
	p.B89S/p.D176V	1	
	p.D176V/p.R246W	1	
	p.D176V/p.R321C	1	
	p.D176V/p.V331A	1	
ED/KD	Total	28	8
	Compound heterozygote	28	8
	p.D176V/p.V572L	12	3
	p.C13S/p.V572L	1	1
	p.D176V/p.I472T	1	1
	p.D176V/p.L603F	1	1
	p.R177C/p.V572L	1	1
	383insT/p.V572L	1	1
	p.D176V/p.G708S	2	
	p.D187G/p.V572L	2	
	p.R8X/p.V572L	1	
	p.D176V/p.G568S	1	
	p.D176V/p.H626R	1	
	p.D176V/p.A630T	1	
	p.I276T/p.V572L	1	
	p.G295D/p.A631V	1	
	p.A600E/p.D176V	1	
KD/KD	Total	30	5
	Homozygote	28	5
	p.V572L homozygote	25	4
	p.M712T homozygote	2	
	p.A630T homozygote	1	
	Compound heterozygote	2	0
	p.V572L/p.R420X	1	1
	1756Gdel (stop)/p.V572L	1	

onset, age at walking with assistance, age at wheelchair use, and current ambulatory status. Initial symptoms included gait disturbance (66.2%, n=47/71), other lower limb symptoms (26.8%, n=19/71), easily fatigued (23.9%, n=17/71), and weakness of hands and fingers (8.5%, n=6/71). In addition, 21.1% (n=15/71) had onset of symptoms before the age of 20. When specifically asked, 47.8% (n=34/71) described themselves as slow runners during childhood, and 42.5% reported having had difficulty with physical exercise during school years.

3.4. Diagnosis

Mean participant age at diagnosis was 33.9±12.6 years (median, 29.5 years; range 17 to 67 years). Mean participant age at first physician visit was 29.6±10.4 years (median, 27 years; range, 12–62 years), and mean time between first visit and diagnosis was 4.4±8.3 years.

3.5. Walking with assistance and wheelchair use

At the time of the survey, 52.0% (n=37/71) were ambulant (41.3±12.8 years); however, only 15.5% (n=11/71, 40.0±13.6 years) could walk without assistance, with the remaining 35.2% requiring assistance (n=25/71, 41.8±12.7 years). Only 7.0% of these participants (n=5/71) could walk up stairs, while 49.3% (n=35/71) were non-ambulant. Wheelchairs were used by 63.6% (23.9% partially bound and 43.7% totally bound) and an electric wheelchair was used by 41.9% (n=31/71). Mean participant age of wheelchair users was 34.9±11.7 years (range, 18–70 years). Wheelchairs were not used by 32.4% (n=26/71) of participants. Current age of wheelchair-free participants was 39.4±12.3 years (range, 21–61 years; median, 34 years) and that of wheelchair-bound participants was 42.8±12.6 years (range, 21–71; median, 42 years).

Kaplan–Meier analysis revealed a median proportional age at walking with assistance of 30.0±1.4 years. Median proportional age of wheelchair users was 36.0±2.7 years, and that for loss of ambulation was 45.0±4.2 years. The time from disease onset to walking with assistance was 7.0±0.4 years, time from disease onset to wheelchair use was 11.5±1.2 years, and time from disease onset to loss of ambulation was 17.0±2.1 years.

3.6. Correlation between disease genotype and phenotype

To determine if a correlation between genotype and phenotype existed, we compared domain mutations (ED/KD, or both) available from medical reports to questionnaire answers (Table 2). Participants with KD/KD mutations (both homozygous and heterozygous) were younger and more severely affected compared to participants with ED/KD or ED/ED mutations. No significant difference in current age or age at disease onset between ED/ED and ED/KD participants was identified. Kaplan–Meier analyses revealed that the proportional time from disease onset to wheelchair use and from disease onset to loss of ambulation was significantly shorter in KD/KD compared to ED/KD participants. ED/ED participants exhibited a shorter time of disease onset to wheelchair use compared to ED/KD participants (Table 3, Fig. 1).

3.7. Comparison between p.V572L homozygous and p.D176V/p.V572L compound heterozygous participants

To compare clinical features in patients with the same mutations, we specifically analyzed data from those with p.V572L (n=25/71, 35.2%) and p.D176V/p.V572L (n=12/71, 16.9%) mutations, as these two were the most frequent mutations in our study population (Table 2). Age at disease onset of homozygous participants (p.V572L) was 21.3±5.7 years (range, 12–32 years) and time from disease onset to wheelchair use was 11.3±5.4 years (range, 3–21 years). Only 16.0% (n=4/25) of these homozygous participants reported that they were not currently using a wheelchair. In contrast, the mean age at disease onset of heterozygous participants (p.D176V/p.V572L) was 35.5±14.1 years (range, 13.5–57 years) and time from disease onset to wheelchair use was 17.9±7.0 years (range, 11–28 years). A total of 66.7% of these compound heterozygous participants (n=8/12) reported that they were not using a wheelchair.

3.8. Questionnaire response compared to medical records

Questionnaires from 17 participants (NCNP outpatient participants) were compared to available medical records (Table 2). Age at disease onset, age at onset of gait disturbance, age at walking with assistance, and age at loss of ambulation were assessed for inter-rater reliability. Age at disease onset, age at onset of gait disturbance, age at walking with assistance, and age at loss of ambulation were assessed for inter-rater reliability. ICC values were 0.979 (95% CI 0.941–0.992) for age at disease onset, 0.917 (95% CI 0.752–0.972) for age at onset of gait disturbances, 0.985 (95% CI 0.949–0.995) for age at walking with assistance, and 0.967 (95% CI 0.855–0.993) for age at loss of ambulation.

4. Discussion

The present study provides a detailed overview of disease severity and progression in 71 Japanese participants with genetically confirmed GNE myopathy. Questionnaire-based surveys have been used to study

Please cite this article as: Mori-Yoshimura M, et al, Heterozygous UDP-GlcNAc 2-epimerase and *N*-acetylmannosamine kinase domain mutations in the *GNE*..., J Neurol Sci (2012), doi:10.1016/j.jns.2012.03.016

Table 2
Comparison of disease course among genotypes.

		Total	ED/ED	ED/LD	KD/KD
Questionnaire	*n*	71	13	28	30
	Age (years old)	43.1 ± 10.7	44.2 ± 11.2	45.3 ± 13.4	40.6 ± 13.0
	Age at onset (years old)	25.5 ± 9.2	26.3 ± 7.3[+]	29.8 ± 11.0[*]	21.2 ± 5.5[*,+]
	Age at walking with assistance	31.8 ± 10.0	34.0 ± 11.1	35.6 ± 10.9[*]	27.8 ± 6.8[*]
	Duration from onset to walking with assistance	8.4 ± 6.5	7.5 ± 7.3	9.2 ± 6.5	8.0 ± 6.6
	Wheelchair user (%)	48 (67.8)	10(76.9)	14 (50.0)[*]	24 (80.0)[*]
	Wheelchair use since (age)	37.6 ± 8.6	36.4 ± 12.0	43.0 ± 8.7[*]	31.2 ± 9.3[*]
	Number of patients with lost ambulation	35 (49.8)	6(46.2)	8 (28.6)[*]	21 (70.0)[*]
	Age at lost ambulation	33.6 ± 9.2	31.2 ± 6.0	39.7 ± 9.5	32.1 ± 9.3
	Duration from onset to loss of ambulation	12.2 ± 5.2	9.8 ± 3.5	13.8 ± 6.4	12.4 ± 5.1
NCNP outpatients	*n*	17	4	8	5
	Age (years old)	43.9 ± 14.1	53.5 ± 8.9[+]	44.3 ± 16.3	35.6 ± 9.2[+]
	Age at onset (years old)	25.8 ± 9.2	33.4 ± 9.2[+]	29.6 ± 13.5	19.6 ± 4.2[+]
	Duration from onset to walking with assistance	7.5 ± 4.2	8.9 ± 5.1	8.1 ± 4.7	5.2 ± 1.5
	Wheelchair user (%)	12 (70.6)	3 (75.0)	4 (50.0)	4 (100)
	Wheelchair use since (age)	33.3 ± 12.6	47.5 ± 17.7	35.2 ± 12.4	25.8 ± 6.3
	Number of patients with lost ambulation	9 (52.9)	3 (75.0)	3 (28.6)[*]	5 (100)[*]
	Age at lost ambulation	33.8 ± 9.3	40.0 ± 0.0	39.0 ± 16.5	31.0 ± 8.2
	Duration from onset to loss of ambulation	10.7 ± 4.2	11.2 ± 5.6	11.1 ± 7.8	6.2 ± 2.6

In the questionnaire group, age at onset and age at walking with assistance were significantly younger in KD/KD patients than in ED/KD patients. The number of wheelchair users and patients with loss of ambulation was significantly higher in the KD/KD group than in the ED/KD group. In contrast, with the exception of age at onset, there were no significant differences between ED/ED and ED/KD or KD/KD patients in these clinical parameters. The ED/ED patients were older than the others, and KD/KD patients tended to show the fastest progression.

[*] $p<0.05$ between ED/KD and KD/KD.

[+] $p<0.05$ between ED/ED and KD/KD.

the natural disease course of other rare neuromuscular disorders, such as Pompe disease [18] and spinal muscular atrophy type-1 [19]. It is difficult to establish the natural history of such rare disorders using medical records only because patients are typically seen in many different hospitals. In the present study, we used a self-reporting questionnaire and support its use for complementing medical records because it provides a more complete disease overview and establishes specific clinical trends or correlations. Indeed, our questionnaire demonstrates excellent inter-rater reliability against medical records and yields several findings regarding differences in disease progression among genetically distinct, GNE myopathy participants.

Only 15.5% of participants could walk and 7.0% could walk up stairs without assistance, which reflects the fact that GNE myopathy patients often require canes and/or leg braces at an early disease stage. This indicates that traditional six-minute walk or four-step walking tests often used to evaluate muscular dystrophies or myopathies can only be applied in a very limited number of cases, such as natural disease course studies or clinical trials. Therefore, alternate evaluation tools are required, which should include functional measurements that can be completed without canes or braces. For example, the Gross Motor Function Measure is a useful tool for evaluating mildly and severely affected patients [20].

The male to female ratio in our study population (27 males and 44 females) was skewed from the expected ratio for autosomal recessive inheritance. However, the male to female ratio of the 17 NCNP outpatient participants was 9:8. One possible explanation for the observed sex ratio in our study population is that female participants tend to be more enthusiastic toward questionnaire-based and/or PADM activities. There was no significant difference in age at survey and age at disease onset between male and female participants. However, in a mouse model of GNE myopathy, weight loss and muscle atrophy were more pronounced and occurred earlier in females compared to males [11].

We showed that KD/KD mutations are associated with a more severe phenotype compared to ED/KD mutations. Indeed, KD/KD participants had an earlier disease onset, a more rapid and progressive disease course, and a shorter time from disease onset to loss of ambulation. This was also observed in the 17 NCNP outpatient participants analyzed in our study. In contrast, ED/ED participants did not show significant differences across disease course parameters analyzed except for an earlier and later age at disease onset compared to ED/KD and KD/KD participants, respectively. Thus, ED/ED participants appear to have a disease severity intermediate between ED/KD and KD/KD participants. One possible explanation is that the major mutation, p.V572L, may be associated with a more severe phenotype. In general, the reasons for this earlier onset and disease progression remain unknown. Jewish GNE myopathy patients with homozygous p.M712T mutations have a milder phenotype compared to Japanese patients, as most of their quadriceps are spared and they usually become wheelchair-bound 15 years or more after disease onset [13,21]. Our study population included two women with homozygous p.M712T mutations: a 38 year-old ambulant and a 35 year-old non-ambulant participant. Although the two participants had a slightly later disease onset (ages 23 and 27 years, respectively) compared to KD/KD participants, the difference was not significant.

An asymptomatic patient with a p.D176V homozygous mutation was previously reported [3]. The study suggested that p.D176V homozygous patients may show a mild or late disease onset phenotype. The results presented here may support this observation as no p.D176V homozygous participants were present in our study

Table 3
Inter-rater reliability of the questionnaire.

	Onset	Age of gait disturbance	Age of gait with help	Age at loss of ambulant
Number of patients	17	17	13	9
ICC (95% CI)	0.979 (0.941–0.992)	0.917 (0.752–0.972)	0.985 (0.949–0.995)	0.967 (0.855–0.993)
p	0.000	0.000	0.000	0.000

Age at onset, age at onset of gait disturbances, age at walking with assistance, and age at loss of ambulation were assessed in a subgroup of 17 outpatients to evaluate the inter-rater reliability of the questionnaire.

Please cite this article as: Mori-Yoshimura M, et al. Heterozygous UDP-GlcNAc 2-epimerase and *N*-acetylmannosamine kinase domain mutations in the *GNE*... J Neurol Sci (2012), doi:10.1016/j.jns.2012.03.016

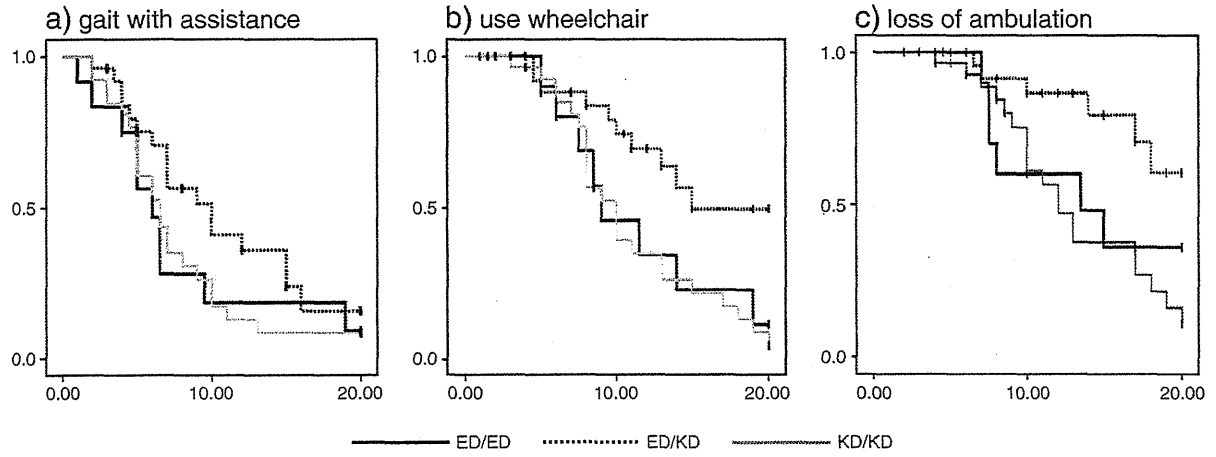

Fig. 1. Kaplan–Meier analysis of time from disease onset to (a) walking with assistance, (b) wheelchair use, and (c) loss of ambulation. Significant differences between ED/KD and KD/KD genotypes were identified. Age at disease onset was significantly different between ED/ED participants and ED/KD and KD/KD participants.

population, although p.D176V was the second most common mutation carried by 29 of our participants. In addition, a high variability was observed regarding age at disease onset and disease progression, underscoring the role of a yet-to-be identified factor(s) in determining disease phenotype.

The recruitment of participants from PADM and highly specialized neurology hospitals is a potential source of selection bias and thus a limitation of this study. These participants are likely to be more motivated because they are more severely affected compared to the general patient population. Furthermore, patients with lower disease severity may not yet be diagnosed with GNE myopathy. Therefore, our study may not accurately reflect the general patient population. Nevertheless, we believe our findings provide important information as our study population covers a broad range in age (22 to 81 years) and symptoms (minimal to wheelchair-bound). Finally, recall bias may also affect results presented in this retrospective study. Therefore, future studies should be performed with an emphasized prospective design.

In conclusion, our study shows that the KD/KD genotype (*i.e.*, p.V572L homozygous mutation) is associated with a more severe phenotype compared to compound heterozygous ED/KD mutations. Because only a small number of participants could walk, future studies should include ambulation-independent motor tests to yield a more comprehensive clinical overview in GNE myopathy patients with different genotypes.

Supplementary data to this article can be found online at doi:10.1016/j.jns.2012.03.016.

Conflict of interest

We certify that there is no conflict of interest with any financial organization regarding the material discussed in the manuscript.

Acknowledgments

We thank members of the Patients Association for Distal Myopathies (PADM) for their help. This work was partly supported by the Research on Intractable Diseases of Health and Labor Sciences Research Grants; Comprehensive Research on Disability Health and Welfare Grants, Health and Labor Science Research Grants; Intramural Research Grant (23-4, 23-5) for Neurological and Psychiatric Disorders of NCNP; and a Young Investigator Fellowship from the Translational Medical Center, NCNP.

References

[1] Nonaka I, Sunohara N, Satoyoshi E, Terasawa K, Yonemoto K. Autosomal recessive distal muscular dystrophy: a comparative study with distal myopathy with rimmed vacuole formation. Ann Neurol 1985;17:51–9.
[2] Argov Z, Yarom R. "Rimmed vacuole myopathy" sparing the quadriceps. A unique disorder in Iranian Jews. J Neurol Sci 1984;64:33–43.
[3] Nishino I, Noguchi S, Murayama K, Driss A, Sugie K, Oya Y, et al. Distal myopathy with rimmed vacuoles is allelic to hereditary inclusion body myopathy. Neurology 2002;59:1689–93.
[4] Eisenberg I, Avidan N, Potikha T, Hochner H, Chen M, Olender T, et al. The UDP-N-acetylglucosamine 2-epimerase/N-acetylmannosamine kinase gene is mutated in recessive hereditary inclusion body myopathy. Nat Genet 2001;29:83–7.
[5] Kayashima T, Matsuo H, Satoh A, Ohta T, Yoshiura K, Matsumoto N, et al. Nonaka myopathy is caused by mutations in the UDP-N-acetylglucosamine-2-epimerase/N-acetylmannosamine kinase gene (GNE). J Hum Genet 2002;47:77–9.
[6] Keppler OT, Hinderlich S, Langner J, Schwartz-Albiez R, Reutter W, Pawlita M. UDP-GlcNAc 2-epimerase: a regulator of cell surface sialylation. Science 1999;284:1372–6.
[7] Malicdan MC, Noguchi S, Nishino I. Recent advances in distal myopathy with rimmed vacuoles (DMRV) or hIBM: treatment perspectives. Curr Opin Neurol 2008;21:596–600.
[8] Noguchi S, Keira Y, Murayama K, Ogawa M, Fujita M, Kawahara G, et al. Reduction of UDP-N-acetylglucosamine 2-epimerase/N-acetylmannosamine kinase activity and sialylation in distal myopathy with rimmed vacuoles. J Biol Chem 2004;279:11402–7.
[9] Broccolini A, Gidaro T, De Cristofaro R, Morosetti R, Gliubizzi C, Ricci E, et al. Hyposialylation of neprilysin possibly affects its expression and enzymatic activity in hereditary inclusion–body myopathy muscle. J Neurochem 2008;105:971–81.
[10] Salama I, Hinderlich S, Shlomai Z, Eisenberg I, Krause S, Yarema K, et al. No overall hyposialylation in hereditary inclusion body myopathy myoblasts carrying the homozygous M712T GNE mutation. Biochem Biophys Res Commun 2005;328:221–6.
[11] Malicdan MC, Noguchi S, Nonaka I, Hayashi YK, Nishino I. A Gne knockout mouse expressing human GNE D176V mutation develops features similar to distal myopathy with rimmed vacuoles or hereditary inclusion body myopathy. Hum Mol Genet 2007;16:2669–82.
[12] Malicdan MC, Noguchi S, Hayashi YK, Nonaka I, Nishino I. Prophylactic treatment with sialic acid metabolites precludes the development of the myopathic phenotype in the GNE myopathy mouse model. Nat Med 2009;15:690–5.
[13] Argov Z, Eisenberg I, Grabov-Nardini G, Sadeh M, Wirguin I, Soffer D, et al. Hereditary inclusion body myopathy: the Middle Eastern genetic cluster. Neurology 2003;60:1519–23.
[14] Tomimitsu H, Shimizu J, Ishikawa K, Ohkoshi N, Kanazawa I, Mizusawa H. Distal myopathy with rimmed vacuoles (DMRV): new GNE mutations and splice variant. Neurology 2004;11:1607–10.
[15] Yabe I, Higashi T, Kikuchi S, Sasaki H, Fukazawa T, Yoshida K, et al. GNE mutations causing distal myopathy with rimmed vacuoles with inflammation. Neurology 2003;12:384–6.
[16] Chu CC, Kuo HC, Yeh TH, Ro LS, Chen SR, Huang CC. Heterozygous mutations affecting the epimerase domain of the GNE gene causing distal myopathy with rimmed vacuoles in a Taiwanese family. Clin Neurol Neurosurg 2007;109:250–6.
[17] Ro LS, Lee-Chen GJ, Wu YR, Lee M, Hsu PY, Chen CM. Phenotypic variability in a Chinese family with rimmed vacuolar distal myopathy. J Neurol Neurosurg Psychiatry 2005;76:752–5.

Please cite this article as: Mori-Yoshimura M, et al, Heterozygous UDP-GlcNAc 2-epimerase and *N*-acetylmannosamine kinase domain mutations in the *GNE*..., J Neurol Sci (2012), doi:10.1016/j.jns.2012.03.016

[18] Hagemans ML, Winkel LP, Van Doorn PA, Loonen MC, Hop WJ, Reuser AJ, et al. Clinical manifestation and natural course of late-onset Pompe's disease in 54 Dutch patients. Brain 2005;128:671–7.
[19] Oskoui M, Levy G, Garland CJ, Gray JM, O'Hagen J, De Vivo DC, et al. The changing natural history of spinal muscular atrophy type 1. Neurology 2007;69: 1931–6.
[20] Sienko Thomas S, Buckon CE, Nicorici A, Bagley A, McDonald CM, Sussman MD. Classification of the gait patterns of boys with Duchenne muscular dystrophy and their relationship to function. J Child Neurol 2010;25:1103–9.
[21] Eisenberg I, Grabov-Nardini G, Hochner H, Korner M, Sadeh M, Bertorini T, et al. Mutations spectrum of GNE in hereditary inclusion body myopathy sparing the quadriceps. Hum Mutat 2003;21:99.

Please cite this article as: Mori-Yoshimura M, et al, Heterozygous UDP-GlcNAc 2-epimerase and *N*-acetylmannosamine kinase domain mutations in the *GNE*..., J Neurol Sci (2012), doi:10.1016/j.jns.2012.03.016

Simple Magnetic Swallowing Detection System

Akihiko Kandori, Toshiyuki Yamamoto, Yuko Sano, Mitsuru Oonuma, Tsuyoshi Miyashita, Miho Murata, and Saburo Sakoda

Abstract—**A magnetic swallowing-detection system that can detect swallowing sounds and measure the distance between two magnetic coils was developed to detect the swallowing function non-invasively. The coils were set on both sides of the thyroid cartilage, and the distance between them changes in accordance with the movement of the thyroid cartilage. Swallowing sounds were detected by a piezoelectric microphone attached to the neck. The coils and microphone were installed in a holding unit that can be positioned at the front of the neck. The system was simultaneously used with videofluorography (VF) to measure nine healthy subjects while they swallowed liquid barium. To evaluate the correlation between the swallowing event detected by the magnetic swallowing-detection system and the swallowing event obtained from VF, two-dimensional positions of the hyoid bone in each VF image were detected. Based on the detection results, the swallowing starting time that was detected by the magnetic swallowing-detection system coincided with that determined from VF, namely, 38±172 ms. The coincidence among the peak time point of VF, that of the distance between the magnetic coils, and that of the swallowing sound appeared to have an intraclass correlation coefficient of 0.9. Correlation between the peak time points of the VF tracking waveforms, the peak time points of distance between the magnetic coils, and the peak timing of the swallowing sound had an intraclass correlation coefficient of 0.9. It can be concluded that the magnetic swallowing-detection system can detect swallowing movements simply and non-invasively without x-ray exposure.**

Index Terms—**Magnetic field, pharynx, swallowing, swallowing sound.**

I. Introduction

THE act of swallowing can be divided into four physiological phases: oral preparatory, oral, pharyngeal, and esophageal [1], [2]. In the oral stage, the tongue plays an important role in processing the food to be swallowed and in transporting the processed food from the oropharynx to the hypopharynx [3]. In the pharyngeal phase, the palatopharyngeus muscle and the stylopharyngeus muscle raise and shorten the pharynx, and the three constrictor muscles (superior, middle, and inferior) contract the pharynx [1]. Ever since videofluorography (VF) investigation of the four-stage mechanism of swallowing was introduced, [4]–[6] VF has been used to study the swallowing mechanism by analyzing, for example, the displacement of the hyoid bone [7], [8] and the size of the bolus [8], [10].

During normal swallowing, the hyoid bone moves along a triangular path: upward, forward, and back to the starting position [2], [11]. It has been reported that the upward displacement in the triangular movement is related primarily to events in the oral cavity, while the forward displacement is related to the pharyngeal processes [7]. Furthermore, a significant difference in the forward displacement of the hyoid bone was found between younger and older subjects [8]. Although the VF patterns have been analyzed to understand the swallowing mechanism, the actual mechanism is still debated due to various complexities that affect it, depending on the type and volume of the bolus [1].

The application of VF recording is limited to patients with abnormalities in swallowing function because it involves x-ray exposure. Several methods to investigate the swallowing function have therefore been developed. Some examples are the use of a non-invasive tool such as a pressure sensor for detecting tongue movement [12], a piezo-electric pulse transducer and EMG electrodes for detecting skin movement [13], impedance pharyngography for detecting electric-impedance changes [14], and a photo-reflective sensor, EMG, and tools to detect swallowing sounds for detecting laryngeal motion [15]. Although these tools provide new information on the swallowing function or dysphasia, they are not as effective as VF for evaluating the swallowing function due to the difficulty in adequately positioning or attaching the electrode.

In this study, a new magnetic electrode-less swallowing-detection system which estimates the length between magnetic coils [16]–[18] and detects swallowing sounds, was developed in order to monitor the swallowing function.

II. Methods

A. Subjects

The swallowing movement of nine normal control subjects (five males; four females; average age: 37±9 years old; age range: 26 to 48 years old) was measured using a magnetic swallowing-detection system and videofluorography (VF) (see Section III). Subjects without a history of neurological problems were defined as the normal controls. Informed consent was obtained from all subjects participating in the evaluation, which was approved by the ethical committee of the National Center Hospital of Neurology and Psychiatry.

Manuscript received July 30, 2011; revised August 21, 2011; accepted August 24, 2011. Date of publication September 08, 2011; date of current version February 08, 2012. The associate editor coordinating the review of this manuscript and approving it for publication was Dr. Subhas Mukhopadhyay.

A. Kandori, Y. Sano, and T. Miyashita are with the Central Research Laboratory, Hitachi, Ltd., Tokyo, 185-8601, Japan (e-mail: akihiko.kandori.vc@hitachi.com, yuko.sano.hd@hitachi.com, tsuyoshi.miyashita.wu@hitachi.com).

T. Yamamoto and M. Murata are with the National Center of Neurology and Psychiatry, Department of Neurology, Tokyo, 187-8551, Japan (e-mail: yamamoto@ncnp.go.jp, mihom@ncnp.go.jp).

M. Oonuma is with the Design Division, Hitachi, Ltd., Tokyo, 107-6323, Japan (e-mail: mitsuru.onuma.ej@hitachi.com).

S. Sakoda is with the Toneyama National Hospital, Osaka 560-8552, Japan (e-mail: sakoda@toneyama.go.jp).

Digital Object Identifier 10.1109/JSEN.2011.2166954